Separation Science and Technology
Publication details, including instructions for authors and subscription information:
http://www.informaworld.com/smpp/title~content=t713708471

Electric Field-Enhanced Coalescence of Liquid Drops

Xiaoguang Zhang[a]; Osman A. Basaran[b]; Robert M. Wham[b]
[a] Department of Chemical Engineering, University of Tennessee, Knoxville, TN [b] Chemical Technology Division, Oak Ridge National Laboratory, Oak Ridge, TN

To cite this Article Zhang, Xiaoguang , Basaran, Osman A. and Wham, Robert M.(1995) 'Electric Field-Enhanced Coalescence of Liquid Drops', Separation Science and Technology, 30: 7, 1169 — 1187
To link to this Article: DOI: 10.1080/01496399508010339
URL: http://dx.doi.org/10.1080/01496399508010339

SEPARATION SCIENCE AND TECHNOLOGY, 30(7-9), pp. 1169-1187, 1995

ELECTRIC FIELD-ENHANCED COALESCENCE OF LIQUID DROPS†

Xiaoguang Zhang
Department of
Chemical Engineering
University of Tennessee
Knoxville, TN 37996

Osman A. Basaran[a]
Robert M. Wham
Chemical Technology Division
Oak Ridge National Laboratory
Oak Ridge, TN 37831-6224

ABSTRACT

A fundamental understanding of drop coalescence and growth is of importance to separations and materials processing. Under external driving forces, drops dispersed in an immiscible fluid collide and coalesce with each other due to their relative motion. As a result of drop coalescence, the average drop size in the dispersion increases over time, improving the separation process. Collision and coalescence of spherical, conducting drops bearing no net charge in dilute, homogeneous dispersions are considered theoretically under conditions where drop motion results from gravity settling and electric field-induced attraction. A trajectory analysis is used to follow the relative motion of two drops and predict pairwise collision rates. A population dynamics equation is then solved to predict the time evolution of the size distribution and the average size of drops. The results show that the rate of drop collision and growth can be increased significantly by applying an electric field, in accord with fundamental experiments and patents on electrocoalescence.

†Research sponsored by the Division of Chemical Sciences, Office of Basic Energy Sciences, U.S. Department of Energy under contract DE-AC05-84OR21400 with Martin Marietta Energy Systems, Inc. Accordingly, the U.S. Government retains a nonexclusive, royalty-free license to publish or reproduce the published form of this contribution, or allow others to do so, for U.S. Government purposes.

*Author to whom correspondence should be sent.

INTRODUCTION

A dispersion of one fluid phase in another, immiscible fluid phase can be separated into two homophases because of the difference in forces being exerted on the two phases, for example, as shown in Figure 1 for a typical gravitationally induced separation process. The initial condition [Figure 1(a)] is a uniform dispersion of drops in an immiscible liquid. After mixing is stopped, the drops begin to fall due to gravity (if the dispersed phase is more dense than the continuous phase). As the drops reach the bottom of the container, they coalesce into an underlying, segregated layer of the dispersed-phase fluid [Figure 1(b)]. This layer grows with time [Figure 1(c)] until all of the dispersed drops have coalesced into it [Figure 1(d)]. During settling, drops collide and coalesce with each other, leading to an increase in the average drop size in the dispersion. As drops coalesce and grow in size, they can be removed from the dispersion by their gravity settling more easily and rapidly than the small drops originally present. Applying an external electric field is a well-known technique to enhance drop collision and coalescence and, therefore, promote the separation rate (1).

In this paper, we present theoretical work to predict the rate of pairwise drop collision induced by combined effects of gravity and electric field-induced forces. We thereby determine the resultant shift in the drop size distribution and increase in the average drop size to quantify the enhancement of drop coalescence by an externally applied electric field. Here, we consider the drops to be perfectly conducting and to bear zero net charge. The drops are assumed to be sufficiently small—typically having diameters of a few hundred microns, or less—that they remain spherical under the action of interfacial tension forces and that inertial forces are negligible compared

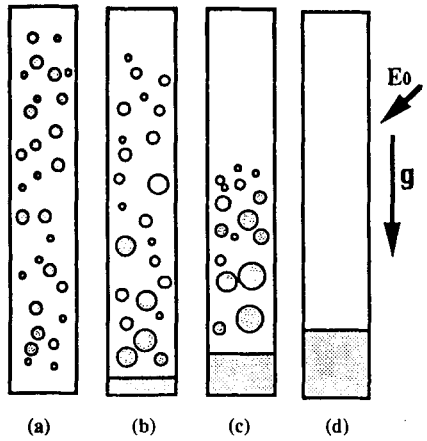

FIGURE 1. Schematic of the phase separation process due to the simultaneous migration and coalescence of falling drops.

to viscous ones. However, the drops are large enough—typically having diameters of a few microns, or more—so that Brownian diffusion is negligible.

Under gravity, drops of different sizes will be in relative motion due to their different settling velocities. The larger drops settle more rapidly than and catch up to the smaller drops in their path, possibly leading to their collisions and coalescence, as illustrated in Figure 2. Application of an external electric field induces charges of the opposite sign on the closest sides of two conducting drops (2). Attraction between the induced charges of the opposite sign on the two nearby drops causes them to approach each other rapidly and increases the possibility of their collision and coalescence, as shown in Figure 2. When two drops are within several radii of each other, the presence of the neighboring drop disturbs the velocity field around each drop. These disturbances bring about an additional hydrodynamic resistance on each drop and cause the drops to flow around each other. If two drops

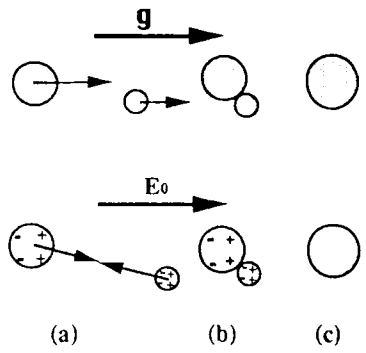

FIGURE 2. Schematic of the process of coalescence of two drops induced by gravity or an electric field: (a) relative motion, (b) collision, and (c) coalescence.

are sufficiently close, van der Waals attraction may also become important: this force can help to pull nearby drops into contact and literally hold them together during coalescence. When the drops come into physical contact, they coalesce into a single, large drop due to the tendency of interfacial tension to minimize the surface area and energy of the drops in contact. As a result of drop collision and coalescence, the drop size distribution in a dispersion will shift toward larger size and the average drop size will increase over time from its initial distribution.

In spite of the relatively widespread use of electric fields as means for improving drop coalescence and phase separations, as reviewed in (1) and (3), a complete fundamental understanding of the enhancement of gravity-induced coalescence of drops by an electric field is lacking because of the complexity of hydrodynamic and electrical interactions among swarms of drops dispersed in a fluid. The purpose of this work is to account for the effects of electric field-induced forces from first principles and thereby predict the coalescence rate under different hydrodynamic and electric conditions.

THEORETICAL DEVELOPMENT

The analysis is restricted to binary interactions and coalescence of a dilute, homogeneous suspension of conducting, spherical drops of viscosity μ_d and density ρ_d dispersed in an immiscible fluid of viscosity μ_o, density ρ_o, and permittivity ϵ. It is assumed that both fluids are Newtonian, and physical properties of these fluids are constant. Drop interfaces are assumed to be free from adsorbed surfactant, and changes in drop sizes—such as by dissolution, diffusion or Ostwald ripening, or breakup—are taken to be negligible over the time scale of coalescence.

In order to predict the temporal evolution of the drop size distribution during a phase separation process, a distribution of drop sizes is discretized into n discrete categories which have equal spacing in the logarithm of drop mass or volume. The resulting population dynamic equation to describe the evolution of this distribution due to drop coalescence is provided by a mass conservation balance on each size category, i (4):

$$\frac{dn_i}{dt} = \frac{1}{2}\sum_{j=1}^{i-1} J_{i-j,j} - \sum_{j=1}^{n} J_{ij}, \tag{1}$$

where n_i is the number of drops of size i per unit volume, t is time, and J_{ij} is the rate of collision per unit volume of drops of size i with drops of size j. The first term on the right-hand side of Eq. (1) is the rate of formation of drops of size i by collisions of two smaller drops (the factor of $\frac{1}{2}$ is to avoid double counting), and the second term is the rate of loss of drops of size i due to their collisions to form larger drops.

The collision rate appearing in Eq. (1) may be expressed as (5)

$$J_{ij} = n_i n_j \pi (a_i + a_j)^2 \mid \underline{\mathbf{U}}_i^{(0)} - \underline{\mathbf{U}}_j^{(0)} \mid E_{ij}, \tag{2}$$

where a_i is the characteristic radius of size category i; $\underline{\mathbf{U}}_i^{(0)}$ is the average velocity of drops of size i due to gravity only; and E_{ij} denotes the collision efficiency, which is defined as a ratio of the actual collision rate to that for rectilinear drop motion due to gravity alone in absence of interactions between drops. Differing from unity, the collision efficiency describes effects of electric field-induced forces, van der Waals attraction, and hydrodynamic interactions on drop collision and coalescence. For binary interactions of drops with radii a_i and a_j undergoing small Reynolds number flow, the external driving forces on each drop balance the hydrodynamic forces, and the velocity, $\underline{\mathbf{V}}_{ij} = \underline{\mathbf{U}}_i - \underline{\mathbf{U}}_j$, of drop i relative to drop j is linearly related to the sum of the external forces and depends only on the instantaneous relative position of the two drops (6). Moreover, the relative velocity can be decomposed into components, one for motion along and another for motion normal to the line-of-centers:

$$\underline{\mathbf{V}}_{ij} = V_{ij}^{(0)}(-L\cos\theta\underline{\mathbf{e}}_r + M\sin\theta\underline{\mathbf{e}}_\theta) - \frac{D_{ij}^{(0)}}{kT}(GF_{E,ij}^{r}\underline{\mathbf{e}}_r - HF_{E,ij}^{\theta}\underline{\mathbf{e}}_\theta) - \frac{D_{ij}^{(0)}}{kT}GF_{V,ij}\underline{\mathbf{e}}_r, \tag{3}$$

where $\underline{\mathbf{e}}_r$ and $\underline{\mathbf{e}}_\theta$ are unit vectors in the radial and tangential directions in a spherical polar coordinate system shown in Figure 3, k is the Boltzmann constant, and T is the absolute temperature. The three terms on the right side of Eq. (3) represent contributions of gravitational forces, electric-field induced forces, and van der Waals attraction on the relative motion of two drops, respectively. The relative velocity for two widely separated drops due to gravity is given by the Hadamard-Rybczynski formula (6, 7):

$$V_{ij}^{(0)} \equiv |\,\underline{\mathbf{U}}_i^{(0)} - \underline{\mathbf{U}}_j^{(0)}\,| = \frac{2(\hat{\mu}+1)(\rho_d-\rho_o)a_i^2(1-\lambda^2)g}{3(3\hat{\mu}+2)\mu_o}, \tag{4}$$

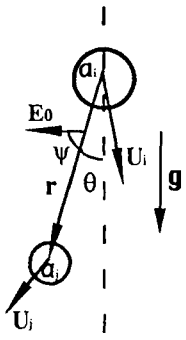

FIGURE 3. Schematic of the coordinate system for the relative motion of two different-size drops.

where $\hat{\mu} = \mu_d/\mu_o$ is the viscosity ratio, $\lambda = a_j/a_i$ is the radius ratio, and g is the magnitude of the gravitational acceleration vector. The relative mobility of two widely spaced drops due to an equal and opposite force, such as the electric field-induced force and van der Waals attraction, is

$$D_{ij}^{(0)} = \frac{kT(\hat{\mu}+1)(1+\lambda)}{2\pi\mu_o(3\hat{\mu}+2)a_i\lambda}. \tag{5}$$

The van der Waals force, $F_{V,ij}$, is generally important only when the drops are very close together and acts along the line-of-centers of the two drops. It is commonly expressed as a gradient of its potential, Φ_{ij} (8):

$$\Phi_{ij} = \frac{A}{6}\left[\frac{8\lambda}{(s^2-4)(1+\lambda)^2} + \frac{8\lambda}{s^2(\lambda+1)-4(1-\lambda)^2} + ln\left(\frac{(s^2-4)(1+\lambda)^2}{s^2(1+\lambda)^2-4(1-\lambda)^2}\right)\right], \tag{6}$$

where A is the composite Hamaker constant and $s = \frac{2r}{a_i+a_j}$ is the dimensionless distance between two drop centers with r denoting the dimensional

Electric field-induced forces on two drops are determined by solving for the distribution of electric field around the drops by means of a bispherical coordinate method (2). The forces are decomposed into two components, along and normal to the line-of-centers of the drops, $F_{E,ij}^r$ and $F_{E,ij}^\theta$, respec-

tively, given by:

$$F^r_{E,ij} = 4\pi\epsilon a_j^2 E_o^2 (F_1 \cos^2\psi + F_2 \sin^2\psi), \tag{7}$$

$$F^\theta_{E,ij} = 4\pi\epsilon a_j^2 E_o^2 F_3 \sin 2\psi, \tag{8}$$

where E_o is magnitude of the external electric field; the force coefficients, F_i (i=1, 2, and 3), are series which depend only on the relative geometry of two drops (i.e., on λ and s); and ψ is the angle that the electric field makes with the vector joining the line-of-centers of the two drops, as shown in Figure 3. In the present work, a horizontal electric field is considered; however, the model is readily extended to predict the influence of an electric field of arbitrary orientation. For a given electric field, the induced forces on two drops are inversely proportional to the fourth power of drop separation (1). Therefore, like van der Waals forces, the electric field-induced forces increase dramatically with decreasing separation between two drops and become an important factor in causing two drops to approach each other only when the two drops are close to one another. In addition, the electric field-induced force increases as the square of the drop size (1), which implies that this force would have a significant effect on large drops. Figure 4 shows the variation of the electric field-induced force, nondimentionalized with $4\pi\epsilon(\frac{a_i+a_j}{2})^2 E_o^2$, on two drops along their line-of-centers as a function of drop separation for different size ratios and $\psi = 0$.

The relative mobility functions [see, e.g., (6)] for motion along the line-of-centers, L and G, and motion normal to the line-of-centers, M and H, describe the effects of hydrodynamic interactions between the two drops. These functions depend on the size ratio of two drops, λ; the viscosity ratio, $\hat{\mu}$; and the dimensionless distance between two drops, s. The complete so-

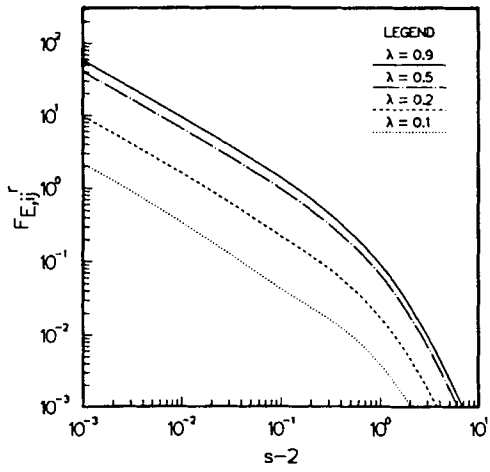

FIGURE 4. Dimensionless electric field-induced force along the line-of-centers of two drops as a function of the dimensionless distance between drop surfaces for ψ=0 and different size ratios.

lutions for the hydrodynamic interactions are obtained using the bispherical coordinate method to solve for velocity fields inside and outside the drops (5, 9, 10). Typical results for L are shown in Figure 5 for different viscosity ratios and $\lambda = 0.5$. Figure 5 shows clearly that the effects of the hydrodynamic interactions increase as two drops approach each other and become significant in resisting the relative motion of two drop as the viscosity ratio increases. It is noteworthy that the hydrodynamic interaction decays slowly as the separation distance between two drops increases and, therefore, possesses longer-range effects on the relative motion of two drops compared to those of electric field-induced forces or van der Waals attraction.

Nondimensionalizing the relative velocity with $V_{ij}^{(0)}$ and dividing the radial component by the tangential component yields a trajectory equation:

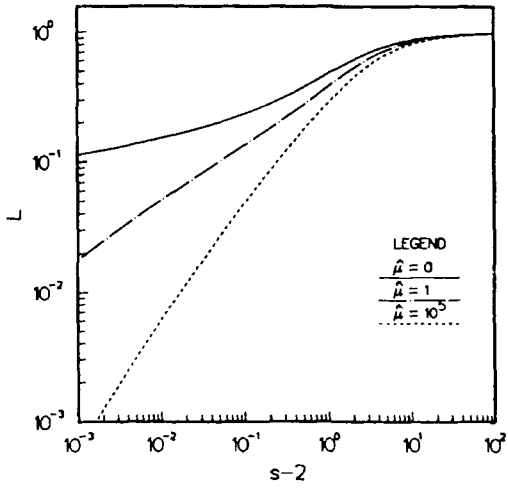

FIGURE 5. Relative mobility function L for two drops in relative motion along the line-of-centers as a function of the dimensionless distance between drop surfaces for λ=0.5 and different viscosity ratios.

$$\frac{ds}{d\theta} = \frac{-L\cos\theta - \frac{G}{Q_{E,ij}}\left(\frac{2\lambda}{1+\lambda}\right)^2\left(F_1\cos^2\psi + F_2\sin^2\psi\right) - \frac{G}{Q_{V,ij}}\frac{a_i+a_j}{2}\nabla\left(\frac{\Phi_{ij}}{A}\right)}{s\left[M\sin\theta + \frac{H}{Q_{E,ij}}\left(\frac{2\lambda}{1+\lambda}\right)^2 F_3\sin 2\psi\right]}, \quad (9)$$

where $Q_{E,ij}$ and $Q_{V,ij}$ are parameters which represent the relative importance of gravitational forces to electric field-induced forces and van der Waals forces, respectively:

$$Q_{E,ij} \equiv \frac{V_{ij}^{(0)}}{\frac{D_{ij}^{(0)}}{kT}4\pi\epsilon\left(\frac{a_i+a_j}{2}\right)^2 E_o^2} = \frac{4(\rho_d-\rho_o)\lambda(1-\lambda)g}{3\epsilon(1+\lambda)^2}\frac{a_i}{E_o^2}, \quad (10)$$

$$Q_{V,ij} \equiv \frac{V_{ij}^{(0)}\frac{a_i+a_j}{2}}{\frac{D_{ij}^{(0)}}{kT}A} = \frac{2\pi\lambda(1-\lambda^2)(\rho_d-\rho_o)g}{3A}a_i^4. \quad (11)$$

$Q_{V,ij}$ is proportional to a_i^4 and is very large compared with unity (5); there-

fore, the contribution of van der Waals forces to the relative motion of drops is small unless the drops are very close to one another. By contrast, $Q_{E,ij}$ depends primarily on the magnitude of the applied electric field and typically ranges from 10^{-2} to infinity.

The trajectory equation is integrated numerically along the drop trajectory from infinite separation of two drops to the point of their collision. Due to interactions between two drops, the drops move along curved trajectories. A so-called limiting trajectory occurs when the relative motion of the drops brings them to a point where contributions from the electric field-induced force and van der Waals attraction just balance that from the gravitational force, as shown in Figure 6. Any relative trajectories which are inside this limiting trajectory end with the drops colliding, whereas those outside the limiting trajectory end with the drops separating. Note that in the absence of inertia, the trajectories do not cross. By comparing the curved limiting trajectories with rectilinear trajectories of two noninteracting drops, the effects of drop interactions on drop coalescence, or the collision efficiency, can be determined (5).

RESULTS AND DISCUSSION

Enhancement of drop collision and coalescence by an electric field are illustrated in Figure 7, which shows the collision efficiency as a function of the strength of the imposed electric field, E_o, which is inversely proportional to the parameter $Q_{E,ij}$, for different size ratios and a typical van der Waals attraction of $Q_{V,ij} = 10^3$ (5). As expected, the collision efficiency increases significantly as the magnitude of the electric field increases, or $Q_{E,ij}$ decreases. The collision efficiency also decreases with decreasing size ratio. This occurs because electric field-induced forces decrease as the size ratio

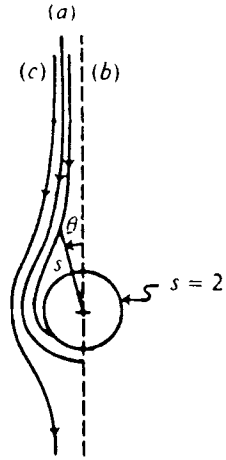

FIGURE 6. Schematic of relative trajectories of two drops: (a) the limiting trajectory, (b) a trajectory terminating with contact, and (c) a trajectory in which two drops move past one another and separate.

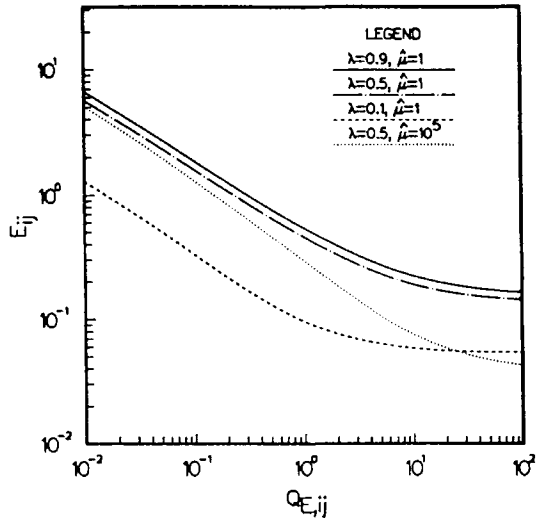

FIGURE 7. Collision efficiency as a function of electric field-induced force parameter, $Q_{E,ij}$, for different size and viscosity ratios with van der Waals force parameter $Q_{V,ij}=10^3$.

decreases (Figure 4) and also because the smaller drop tends to follow the streamlines of the flow and move around the larger one: hence, collision does not occur unless the smaller drop is on a streamline which is very close to the larger drop. Moreover, Figure 7 demonstrates effects of hydrodynamic interactions, which are characterized by the viscosity ratio, $\hat{\mu}$, on drop collision. As the viscosity of the drop phase increases, the resistance experienced by the drops in squeezing the fluid out of the gap separating them increases, resulting in a decrease in the possibility of collision of the two drops. The influence of hydrodynamic interactions is especially pronounced when the electric field-induced forces are small. The influence of electric field on drop collision can be perceived directly from the limiting relative trajectories of two drops, which are shown in Figure 8 for drops of $\lambda = 0.5$ and $\hat{\mu} = 1$ with $Q_{V,ij} = 10^3$ and different $Q_{E,ij}$ values. Two drops under the influence of strong electric field-induced attraction are pulled together rapidly, even when the drops are at large initial distances from the vertical axis of symmetry, compared to those under the influence of weak electric attraction, resulting in a large collision efficiency.

In order to gain a better understanding of the drop collision process, the collision efficiency of the commonly used system of water drops dispersed in 2-ethyl-1-hexanol (11) was calculated. The collision efficiency for this system as a function of the larger drop size is shown in Figure 9(a) with $\lambda = 0.5$ and for various electric field strengths. Again, the collision efficiency is seen to increase as the strength of the electric field increases. Moreover, the collision efficiency is increased for smaller drops over larger drops due to the increased importance of the attractive electric field-induced forces and van der Waals forces relative to gravitational forces. Figure 9(b) shows similar results, but with the collision rate divided by $n_i n_j$. In addition to

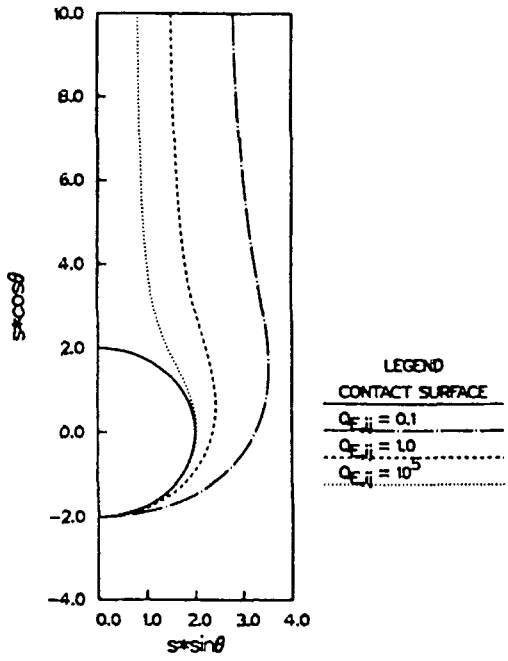

FIGURE 8. Limiting relative trajectories of two drops for λ=0.5 and $Q_{V,ij}=10^3$ with different electric field-induced force parameters.

increasing with increasing electric field strength, the collision rate is seen to increase significantly with increasing drop size, a result that accords with the definition of the collision rate by Eq. (2).

The growth of a population of water drops in a homogeneous, isotropic dispersion of 2-ethyl-1-hexanol was studied by solving the population balance equation, Eq. (1), using the method developed by Berry and Reinhardt (12). The earlier calculated results for the collision rate shown in Figure 9(b) were applied in computations to determine the evolution of a population of drops. Figure 10 shows typical drop size distributions that result after 30 s of drop coalescence for a 1% (by volume) dispersion of water drops in 2-ethyl-1-

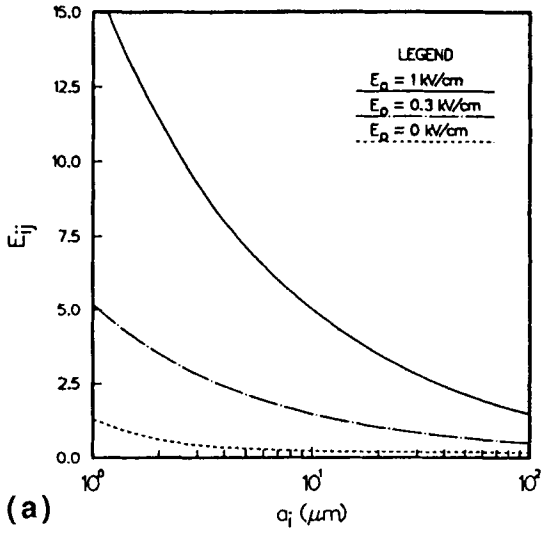

FIGURE 9(a). Collision efficiency for two water drops in 2-ethyl-1-hexanol as a function of the radius of the larger drop for λ=0.5 and various electric field strengths.

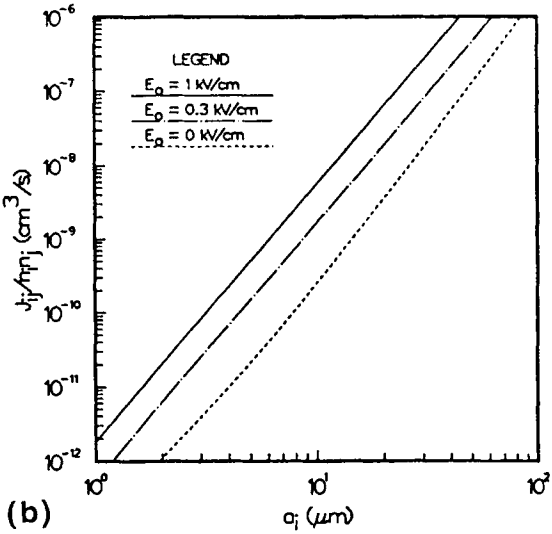

FIGURE 9(b). Collision rate of two water drops in 2-ethyl-1-hexanol as a function of the radius of the larger drop for λ=0.5 and various electric field strengths.

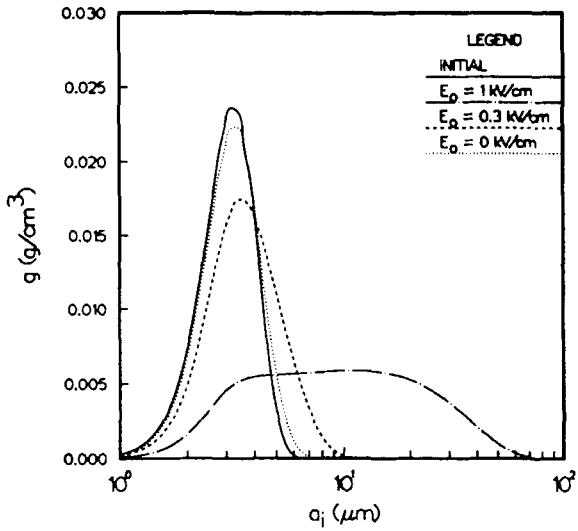

FIGURE 10. Drop size distribution for a water-2-ethyl-1-hexanol system for different electric field strengths after 30 s of coalescence of an initial distribution.

hexanol subject to the conditions of Figure 9. The initial size distribution was chosen to be a normal distribution with a number-average radius of 2 μm and standard deviation of 1 μm and was discretized into size categories for which the drop mass doubles every fourth category. The function, g, plotted in Figure 10 is defined such that

$$\int_0^\infty g(\ln a) d \ln a = \phi, \tag{12}$$

where ϕ is the total volume fraction of the drop phase.

The results shown in Figure 10 indicate that due to the imposed electric field, the initial peak of the size distribution gives way to a second peak which rapidly shifts toward larger sizes after 30 s of drop coalescence. The larger spread in the evolved drop size distribution in the presence of the

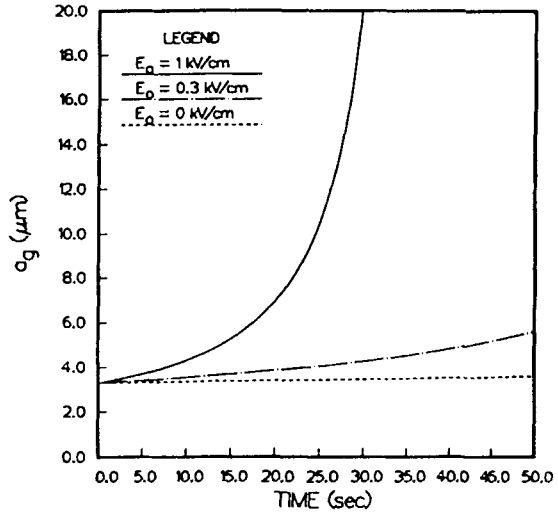

FIGURE 11. Time evolution of mass-averaged drop radius for a water-2-ethyl-1-hexanol system for various electric field strengths.

larger electric field is due to the combined effects of the stronger dependence of the collision rate on the size and size ratio. In other words, drop growth is dominated by collisions between drops of large sizes and moderate size ratios, as discussed earlier. The mass-averaged drop radius is shown in Figure 11 as a function of time for this system, which further reinfores the enhancement of drop growth by an external electric field.

SUMMARY

Detailed quantitative predictions of collision and coalescence rates of two conducting, spherical drops and growth of a population of drops induced by gravitational and electric field-induced forces are presented in this paper for the first time. Using a trajectory analysis to follow the relative motion of pairs of drops, predictions are made of the rate of pairwise drop collisions.

A dynamic population balance equation is then solved to determine the time evolutions of the drop size distribution and the average size in a dilute dispersion due to drop coalescence. The results show that the collision rate increases significantly and the drop growth increases rapidly by imposing an external electric field. Moreover, the results show that the enhancement of drop collision and coalescence due to an electric field is more striking for larger drops.

The model presented here may be used to predict collision and coalescence of conducting, spherical drops under different processing conditions, namely varying strengths and orientations of the imposed electric field, properties of the liquid-liquid system, and the relative geometry of drops. The method can also be extended to more complicated cases. For example, collision and coalescence of drops bearing net charge under an electric field can be readily studied by a straightforward extension of the analyses of this paper. Moreover, experiments to study drop collision and coalescence under gravity and electric field are under development to verify the theoretical predictions.

ACKNOWLEDGEMENTS

This research was sponsored by the Division of Chemical Sciences, Office of Basic Energy Sciences, U.S. Department of Energy under contract DE-AC05-84OR21400 with Martin Marietta Energy Systems, Inc.

REFERENCES

1. L. C. Waterman, Chem. Eng. Prog. 61, 51 (1965).
2. M. H. Davis, Quart. J. Mech. Appl. Math. XVII, 499 (1964).
3. K. J. Ptasinski and P. J. A. M. Kerkhof, Sep. Sci. Technol. 27, 995 (1992).

4. J. R. Rogers and R. H. Davis, J. Atmos. Sci. 47, 1057 (1990).

5. X. Zhang and R. H. Davis, J. Fluid Mech. 230, 479 (1991).

6. S. Kim and S. J. Karrila, Microhydrodynamics: Principles and Selected Applications, Butterworth-Heinemann, Boston (1991).

7. H. Lamb, Hydrodynamics, Dover, New York, 600 (1954).

8. Hamaker, H. C., Physica 4, 1058 (1937).

9. S. Haber, G. Hetsroni, and A. Solan, Int. J. Multiphase Flow A1, 57 (1973).

10. A. Z. Zinchenko, Prikl. Mat. Mech. 44, 30 (1981).

11. O. A. Basaran, T. C. Scott, and C. H. Byers, AIChE J. 35, 1263 (1989).

12. E. X. Berry and R. L. Reinhardt, J. Atmos. Sci. 31, 1814 (1974).